Int. J. Rock Mech. Min. Sci. & Geomech. Abstr. Vol. 28, No. 6, pp. 527–533, 1991
Printed in Great Britain.

0148-9062/91 $3.00 + 0.00

Technical Note

On the Fractal Character of Rock Surfaces

M. SAKELLARIOU†
B. NAKOS†
C. MITSAKAKI†

INTRODUCTION

The roughness of rock surfaces, as is well-established, is an important factor in a variety of rock mechanics problems such as, shear strength [1], flow of water [2] and deformation behaviour [3]. Its significance is also important in geophysical problems related to tectonic faults [4]. Dieterich [5] proposed a constitutive law of frictional behaviour, according to which the coefficient of friction is dependent on a displacement parameter affected by the roughness of surfaces. Based on this Tullis [6] suggested the use of roughness, expressed as a "length" quantity, in order to establish a scaling law for the study of *in situ* phenomena from small-scale samples in the laboratory. Roughness, as a parameter in the above-mentioned problems, causes a scale effect behaviour [7].

The roughness, induced by natural processes, may be considered as a description of the deviation from a smooth line or surface of Euclidean space. Fractal geometry provides an appropriate theoretical model to study the complicated geometry of natural objects in contradiction to Euclidean geometry which utilizes a more simplified approach [8].

The idea of examining the possible fractal character of the 10 typical profiles suggested by ISRM [9], has already been carried out by several researchers (see for example [10–14]). The major advantage of such studies is based on the fact that these profiles offer the possibility to correlate their classification as required by rock mechanics with their geometric description as provided by fractal geometry.

Some drawbacks observed in previous studies are also discussed here.

FRACTAL GEOMETRY

B. Mandelbrot studied sets of mathematical functions of both geometric and stochastic character which he called fractal sets [8]. He showed, using computer graphic representations, that random fractal sets may be used as statistical models in order to simulate a wide range of natural phenomena, from topographic relief to percolation. The basic characteristic of both non-random and random fractal functions is that, although continuous, they are not differentiable at any point, at least for a certain range of scale changes [8].

The fractal sets are characterized by their fractal dimension D. Mandelbrot defines a fractal as a set with a fractal dimension D that lies between the topological D_T and Euclidean one D_E ($D_T < D < D_E$).

The fractal dimension may describe the roughness of a phenomenon or, equivalently, the degree that its projection fills the Euclidean space R^E. Thus, a vertical cut through a relief has a fractal dimension between 1 and 2, while the fractal dimension of a surface lies between 2 and 3.

An important property of many fractal sets is their invariance to similarity transformations (isotropic rescaling of lengths). These fractal sets are called self-similar. For such a set, points $\mathbf{x} = (x_1, x_2, \ldots, x_E)$ in E-dimensional space transform into new points $\mathbf{x}' = (rx_1, rx_2, \ldots, rx_E)$, under the same value of scaling ratio r [15].

Still, for several fractal sets of interest, self-similarity does not apply. However, these sets are invariant to a more general form of transformation, the affine transformation, and they are called self-affine fractals. A point of such a fractal set $\mathbf{x} = (x_1, x_2, \ldots, x_E)$ in E-dimensional space is transformed by an affine transformation into a new point $\mathbf{x}' = (r_1 x_1, r_2 x_2, \ldots, r_E x_E)$, where the scaling ratios $\mathbf{r} = (r_1, r_2, \ldots, r_E)$ are not all equal [15]. The fractal dimension of a self-affine fractal is not uniquely defined [15–17]. Its global value is $D = D_T$, that is a self-affine fractal is not fractal globally. But a local fractal dimension can be computed according to the standard procedure. This behaviour of a self-affine fractal set involves a cross-over value of the sample interval, where the local value of the fractal dimension passes to the global one [16,17]. Clearly self-affinity is a generalization of self-similarity.

The characteristic relation for the fractal dimension D, that expresses the property of self-similarity is [8]:

$$D = \frac{\log(N)}{\log[1/r(N)]}, \tag{1}$$

where $r(N)$ is the similarity ratio and N is the number of non-overlapping, self-similar parts comprising the fractal set, dependent on the similarity ratio.

The relation is used in order to compute D for lines (or surfaces) created by purely geometric generators as

†Faculty of Rural and Surveying Engineering, National Technical University of Athens, 9 Heroon Polytechniou Str., 157 73 Zographos, Greece.

shown in Fig 1. The unit length in (a) is divided with similarity ratio $r(N) = 1/4$. The fractal curve in (b) comprises $N = 8$ parts, while in (c) the procedure is repeated with $r(N) = 1/16$ and $N = 64$ parts. The fractal dimension of such a line, according to (1), is $D = 1.5$.

The exactly self-similar Von Koch curve (Fig. 1) is only a crude model of a coastline and it differs in one significant aspect. Upon magnification, segments of a real coastline look like—but are never exactly like—segments at different scales. The concept of fractal dimension, however, can also be applied to such statistically self-similar objects as the coastlines. This property of statistical self-similarity (or self-affinity) is the central feature of fractals in nature [18].

A topographic relief or a fracture surface appears to behave as random fractal set [8,11,17–19]. Vertical cuts (profiles) through such surfaces are statistically self-affine fractals with a local fractal dimension lying between 1 and 2 [16–18]. However, horizontal cuts of these surfaces give rise to coastlines (isarithmic lines) which are indeed statistically self-similar and have a unique fractal dimension D $(1 < D < 2)$. Therefore a unique value for the fractal dimension of the surface (D_S) can be derived as $D_S = D + 1$ [17].

METHODS FOR COMPUTING FRACTAL DIMENSION

All computational methods involve the estimation of parameters of various statistical functions and data sampled over lines or surfaces. Such samples should cover a range of scales as broad as possible. In each method, the final step of the procedure is the least-squares estimation of the slope of a linear model fitted to the data of a double logarithmic diagram. Both the verification of the fractal character of a line (or a surface) and the reliability and the statistical significance of these parameters should be statistically checked, using a high confidence level [19].

Depending on whether one deals with self-similar fractal sets, as the isarithmic lines of a fractal surface, or self-affine ones, as the profiles of this surface, the fractal dimension may be estimated by four methods.

Two statistical methods, namely spectral and variance analysis, have already been used extensively in order to describe the fractal behaviour of self-affine fractal sets, such as the profiles of the topographic relief or of a rock fracture surface [4,11].

For self-similar fractal sets, two geometric methods for determining the fractal dimension are available, one that correlates the length of a line to the sampling step size [and substitutes equation (1) in the case of statistical self-similarity] and the other based on the correlation between the perimeter and the area of closed curves [18].

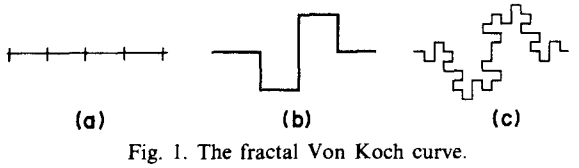

Fig. 1. The fractal Von Koch curve.

All four methods involve expressions of a power law. The relations for fractal lines $(1 < D < 2)$, whose logarithmic expression is the final step of each method, are given below:

(a) length L to sampling step size ϵ:

$$L(\epsilon) \approx \epsilon^{1-D}; \tag{2}$$

(b) area A to perimeter P:

$$A(\epsilon) \approx P(\epsilon)^{2/D}; \tag{3}$$

(c) normalized variance function V_z vs correlation distance d:

$$\frac{V_z(d)}{\sigma_z^2} \approx d^{4-2D} \text{ where } V_z(d) = E\{(z_i - z_j)^2\}, \tag{4}$$

with σ_z^2 the variance of each sample, where the sample size depends on the choice of the correlation distance d, between points i and j;

(d) power spectrum $G(\lambda)$ vs wavelength λ:

$$G(\lambda) \approx \lambda^{5-2D}. \tag{5}$$

There are certain aspects that should be considered when the fractal dimension is used as a geometric parameter in order to describe the "roughness" of natural phenomena.

Probably, the most important one is the clarification that self-affinity (anisotropic or direction-dependent rescaling) does not preclude scale invariance and, thus, fractal behaviour [16,17]. Nevertheless, the rather hazy conception that only self-similarity establishes fractal behaviour is found in papers dealing with rock mechanics applications [12].

Profiles of a rock joint surface seem to behave as statistically self-affine fractals. Methods, such as method (a) mentioned above (and all variations such as the Cantor method, grid method etc. [12–14]) will result in identical estimations of fractal dimension D, only in the case of self-similar fractals (horizontal cuts of a rock surface), a conception that is well-established theoretically [16,17]. These methods may be used mechanically for affine fractals, but the fractal dimension estimates will depend heavily on the position of the critical cross-over value along the x-axis, in other words these estimates will depend on the units of the (x, y)-axes. The same problem will emerge when using methods (c) and (d), but they should be preferred, since the raw data of a profile are better described by such statistical models [18,20]. Values of correlation distance, d or wavelength λ approaching the total sample length result in bending the best fitting line of the log–log diagram. An estimation of the fractal dimension using only this second part of the diagram will tend to its global value, that is $D \to D_T$.

Another topic regarding the raw data collected from *in situ* measurements of a rock joint surface is also important. It should be noted that data sampled along profiles, even if these profiles span both x-, y-directions of the surface in a local Cartesian system, are 1-D and should be treated as such. Furthermore, since a rock

joint surface $Z(x, y)$ may well be considered as a natural phenomenon of random character, profiles of such a surface are often approached as random stationary processes [21]. What may be assumed as stationary here are the increments $(z_i - z_j)$, [equation (4)], which are considered as having a Gaussian distribution with zero mean value and variance given by the expression in method (c), dependent only on the correlation distance d. The random field of the fractal surface itself $Z(x, y)$, has also stationary increments and, furthermore, the points (x, y) lie in an isotropic plane, where all positions and directions are considered statistically equivalent.

Thus, horizontal cuts provide a collection of islands' coastlines which are unbounded self-similar (isotropic rescaling) and have only one common dimension, which is the local dimension of the profiles. In other words, horizontal cuts are not at all affected by global quantities, in contrast to the profiles, since their intrinsic scale is infinite [17].

Methods similar to the ones used for topographic relief would provide real 2-D data of the rock surface in the form $z_i\ (x_i, y_i)$. In that case, 2-D expressions of the normalized variance function and power spectrum could be used, but such an approach is particularly demanding in modelling, due to the presence of anisotropy [22]. Creating a digital terrain model (DTM) of the rock surface in a computer, plotting isarithmic lines and applying method (b) for self-similar fractals (since the x- and y-directions of the surface rescale under the same scaling ratio) is the most stable and least ambiguous approach when 2-D data are available [11,18–20].

APPLICATIONS

The results of two applications are presented here in order to verify the fractal character of the samples and to estimate their fractal dimension. The first application deals with the 10 typical roughness profiles suggested by ISRM [9]. The second one deals with two rock joint surfaces after *in situ* direct shear testing.

Both statistical verification of the fractal character and the estimation of the fractal dimension of a set of points can be carried out by applying one of the four methods described above. Regarding the verification of fractal behaviour, two statistical tests are suggested [19], based on the parameters of the linear model that fit the data in the log–log space. In the first one, the value of the correlation coefficient ρ is checked with the null hypothesis: $H_0(\rho \neq 1)$ at 99% confidence level [23]. In the second statistical test, the value of the slope b against the equivalent value for a Euclidean shape or surface b_E is checked by rejecting the null hypothesis: $H_0\ (b = b_E)$ at 95% confidence level [23]. If the samples pass these two tests, they can be accepted as fractal sets in a statistical sense. At last a third test, regarding the significance of the slope b and, thus of the fractal dimension D of the sample, must be carried out. The null hypothesis in this case is: $H_0\ (b = 0)$ at 99% confidence level [23].

As mentioned above, the profiles are rescaling under affine transformations, in other words, these profiles can be treated as self-affine fractal sets, so methods (c) and (d) must be used in order to verify the fractal character of the 10 profiles and to estimate their fractal dimension.

Table 1. Results of the regression between the normalized variance function and correlation length for the 10 typical roughness profiles of ISRM

Profile	b	D	ρ
01	1.014 ± 0.002	1.493 ± 0.001	0.9996
02	0.962 ± 0.004	1.519 ± 0.002	0.9994
03	1.281 ± 0.012	1.360 ± 0.006	0.9980
04	0.957 ± 0.006	1.522 ± 0.003	0.9961
05	1.306 ± 0.003	1.347 ± 0.001	0.9995
06	1.669 ± 0.002	1.166 ± 0.001	0.9998
07	1.585 ± 0.005	1.208 ± 0.002	0.9996
08	1.765 ± 0.002	1.118 ± 0.001	0.9999
09	1.565 ± 0.005	1.218 ± 0.003	0.9996
10	1.624 ± 0.007	1.188 ± 0.004	0.9996

At first, the 10 profiles were digitized, in order to acquire the raw data for the samples. The 10 typical roughness profiles as source figures were digitized with a scanner using a resolution of 85 μm. Next these raw data were transformed from raster to vector form using available software [19]. For each method, namely (c) and (d), two respective routines were developed in order to verify the fractal character and estimate the local fractal dimension of the 10 ISRM profiles. The calculation of the power spectrum is based on the algorithm of Cooley *et al.* [24].

Table 1 summarizes the results of the regression the between normalized variance function and correlation length for each profile. All tests for the 10 profiles passed successfully. It can be seen (Table 1) that the first five profiles (1–5) have relatively high values of their estimated fractal dimension D. For the rest (6–10), the

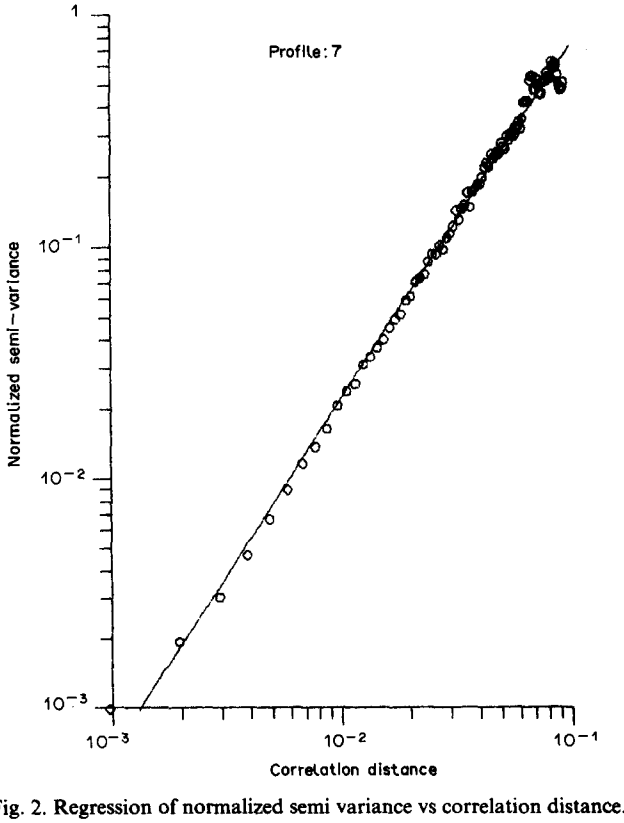

Fig. 2. Regression of normalized semi variance vs correlation distance.

estimated values of the fractal dimension D follow the ISRM roughness classification (Fig. 2).

The final remark is that only the fractal character can be detected regarding these 10 typical roughness profiles. The erractic behaviour of the first five profiles may be explained by the quality of source material (smooth figures of a book) that causes mixing of noise in the signal in the raw data, a fact that cannot be overcome.

The same behaviour is even more pronounced in all profiles after regression between the power spectrum and wavelength (Fig. 3).

Next, the area to perimeter method was carried out for two rock joint surfaces, from the same site after *in situ* shear testing, since, as it has already been stated in applications from other fields (i.e. cartography [19]), it is more stable and less ambiguous. In this case, the samples were examined under the property of self-similarity.

The raw data have the form of a digital model of a joint surface, like a DTM (Fig. 4a). Next, horizontal cuts of the joint surfaces should be created by plotting contour lines from the DTM (Fig. 4b).

Table 2 summarizes the results of the regression between area and perimeter for these two samples (Fig. 5). All tests passed successfully. It can be seen (Table 2), that the two joint surfaces may be accepted as fractal sets in a statistical sense.

DISCUSSION—CONCLUSIONS

Roughness profiles appear to behave as self-affine random fractal sets, at least for a certain rather broad range of scales. Thus, rescaling of a roughness profile sample is possible, providing that a reliable and statistically significant estimation of D is made. At this point, it should be emphasized once more, that in the case of self-affine random fractal sets, as the profiles, one must distinguish between local D_L and global D_G fractal dimension, with the latter one tending to the topological dimension, $D_T = 1$.

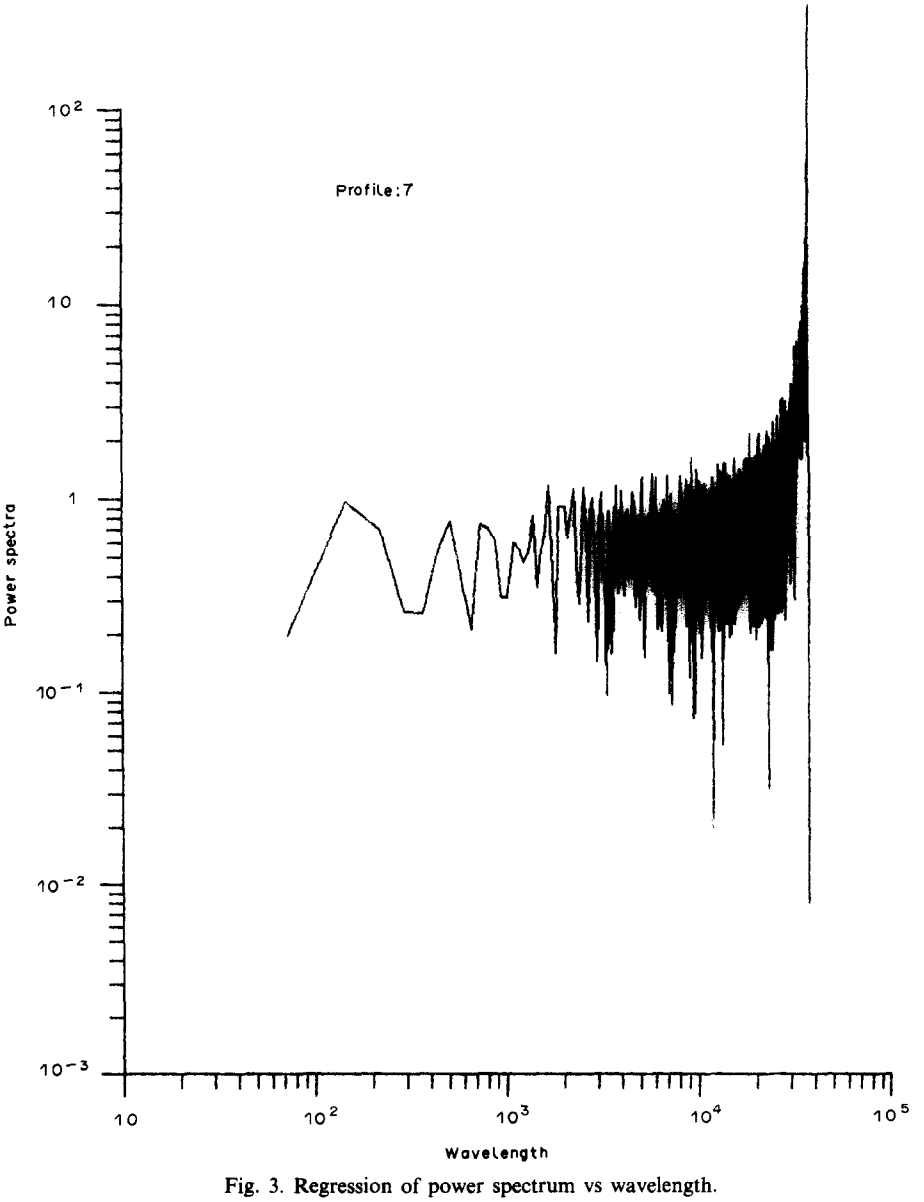

Fig. 3. Regression of power spectrum vs wavelength.

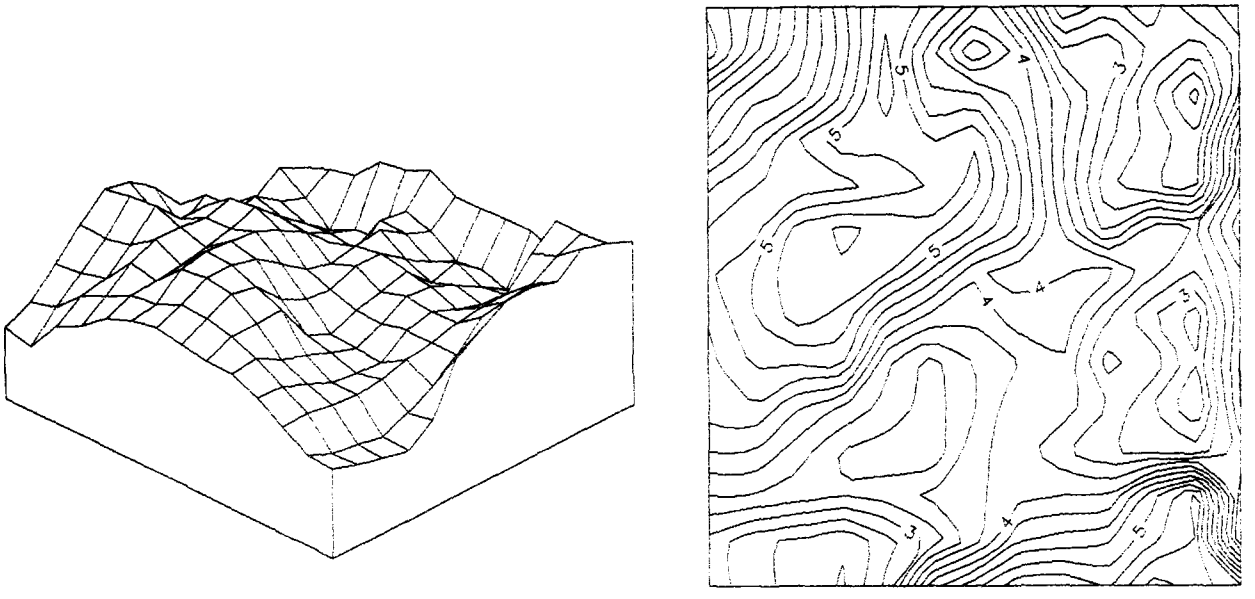

Fig. 4. Digital model of a rock joint surface: (a) axonometric view; and (b) isarithmic lines. Contour interval = 0.25 mm.

Table 2. Results of the regression between area and perimeter for the two rock joint surfaces after *in situ* shear testing

Rock	b	D	ρ
1	1.840 ± 0.065	1.087 ± 0.038	0.9932
2	1.818 ± 0.094	1.100 ± 0.057	0.9819

Expression (1), or other equivalent forms like equation (2), all valid for self-similar fractal sets, have been used in estimating the fractal dimension of the 10 ISRM profiles [11–14]. It was observed that if these profiles were considered as fractal sets, the respective D-values seemed to conform to the profiles' order in the "roughness scale", as shown in Table 3, although these D-values were very close to unity, located in the interval $1.0003 < D < 1.01$. In all cases (Table 3), it seems that these D-values approach the global dimension $D_G \rightarrow D_T = 1$ of the profiles. If rather large yardstick lengths, compared to the curve's undulations, are used to trace the length of a profile, the length measured in effect is that of an almost horizontal line ($D \rightarrow D_T = 1$), since the yardstick walked along the curve remains mostly parallel to the x-axis [16,17] (Fig. 6). Obviously, this effect is more pronounced for the smoother profiles, as shown in Table 3. On the other hand, when progressively smaller yardsticks are used the better tracing of the real length of the profile is possible. This dependence of the D-values on the choice of the yardstick length was also reported [12]. Thus, if the intrinsic properties of self-affine fractals are taken into account, all the above-mentioned observations verify the random self-affine fractal character of the 10 roughness profiles.

In such cases, methods like the ones used in this paper, and especially the normalized variance function, should be preferred, since the increments $(z_i - z_j)$ which describe

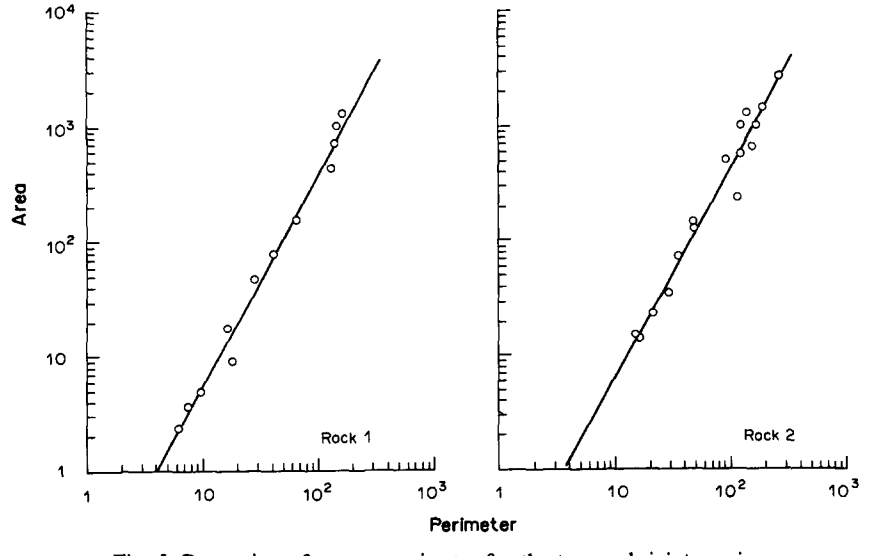

Fig. 5. Regression of area vs perimeter for the two rock joint specimens.

Table 3. Comparison of results between Refs [11, 12, 14] using equation (1)

JCR range	Fractal dimension		
	Sakellariou *et al.* [11]	Lee *et al.* [14]	Maerz and Franklin [12]
0–2	1.0003	1.0005	
2–4	1.0009	1.0017	
4–6	1.0013	1.0028	1.0029 (Fig. 8)
6–8	1.0032	1.0039	
8–10	1.0032	1.0044	
10–12	1.0042	1.0056	
12–14	1.0059	1.0071	
14–16	1.0081	1.0081	
16–18	1.0074	1.0096	
18–20	1.0123	1.0134	1.017 (Fig. 7)

better the deviation of the curve from a smooth one, are used and, furthermore, in a second-order power form [equation (4)]. Such methods are more sensitive to the discrimination between the local and global values, but the dependence on the yardstick length is again present, as an inherent behaviour of self-affine fractal sets.

The results given in Table 1 appear controversial since they do not agree with common sense in classifying the suggested profiles according to their roughness. Thus, the first profile, being almost a straight line, has a D-value much greater than the value of the tenth one, which seems to be rougher. The rougher profiles have, in general, smaller D-values, much closer to the unique and reasonable values derived by the stable area to perimeter method (Table 2). This behaviour can be explained by the fact that the noise-to-signal ratio introduced by the digitization with the scanner, affects more the $(z_i - z_j)$ increments of the "smooth" profiles than of the "rough" ones. Since the variogram method exaggerates these increments, the erratic ones introduced to the "smooth" profiles give rise to unrealistic D-values while, for the "rough" profiles, the presence of the real increments overcomes the influence of the erratic ones, and the method provides more reasonable results.

The above discussion may lead to the conclusion that the ISRM profiles should be considered as random self-affine fractal sets. This concept is in agreement with the "scale effect" observed in the behaviour of rock discontinuities. Barton *et al.* [3] and Bandis *et al.* [7] have observed that for the shear strength of rock joint surfaces the following law is valid:

$$\frac{\mathrm{JRC}}{\mathrm{JRC}_0} = \frac{\bar{\alpha}}{\bar{\alpha}_0} = \left[\frac{L}{L_0}\right]^{-0.02\mathrm{JRC}_0}, \tag{6}$$

where JRC is the joint roughness coefficient, $\bar{\alpha}$ is the mean inclination angle to asperities based on a 2% stepsize and L is the specimen's length. The subscript (0) indicates the reference conditions for the laboratory scale.

This experimentally observed behaviour is in qualitative agreement with the fact that if unique D-values could be estimated for the ISRM profiles, these profiles would obey the following self-affine scaling law [11,25]:

$$\frac{z}{z_0} = \left[\frac{L}{L_0}\right]^{2-D}, \tag{7}$$

where z is the height increment of the profile for a certain correlation distance L.

Or equivalently:

$$\frac{\tan\alpha}{\tan\alpha_0} = \left[\frac{L}{L_0}\right]^{1-D} \tag{8}$$

where α is the tilt angle corresponding to correlation distance L.

Unique D-values for the above expressions could be estimated by the area to perimeter method, providing that a DTM for each respective rock joint surface is available. Thus, each ISRM profile would be accompanied by a unique local fractal dimension D_L, as a roughness measure, and a more objective criterion for roughness classification would be available.

For practical purposes, sampling of rock joint profiles from *in situ* measurements should be carefully planned, so that several profiles—and for a broad range of sampling intervals from very short to long wavelengths—should be collected. Analysis of these data as suggested here should follow and the derived local fractal dimension D_L should be compared to the ones referring to the 10 typical ISRM profiles.

In conclusion, the roughness scale effect, observed in both laboratory experiments and *in situ* observations, where profiles of rock joint surfaces are used as samples, may be explained by fractal geometry, since this effect is due to the fact that profiles obey the more general scaling law of self-affinity.

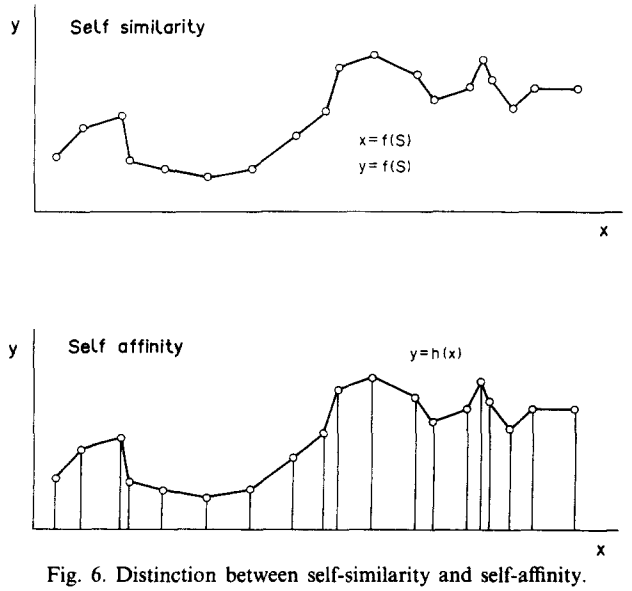

Fig. 6. Distinction between self-similarity and self-affinity.

Accepted for publication 27 February 1991.

REFERENCES

1. Goodman R. E. *Methods of Geological Engineering*, p. 472. West, St Paul, Minn. (1976).
2. Brown S. R. Fluid flow through rock joints: the effect of surface roughness. *J. Geophys Res.* **92,** 1337–1347 (1987).
3. Barton N., Bandis S. and Bakhtar K. Strength, deformation and conductivity coupling of rock joints. *Int. J. Rock Mech. Min. Sci. & Geomech. Abstr.* **22,** 121–140 (1985).
4. Brown S. R. and Scholz C. H. Broad bandwidth study and the topography of natural rock surfaces. *J. Geophys. Res.* **90,** 12,575–12,582 (1985).
5. Dieterich J. H. Modeling of rock friction 1. Experimental results and constitutive equations. *J. Geophys Res.* **84,** 2161–2168 (1979).
6. Tullis T. E. Friction and faulting, Editor's Note. [In *Friction and Faulting* (Edited by T. E. Tullis), Birkhauser Verlag (1987)]. Reply: *Pure Appl. Geophys.* **124,** 375–381 (1986).
7. Bandis S., Lumsden A. C. and Barton N. R. Experimental studies of scale effects on the shear behaviour of rock joints. *Int. J. Rock Mech. Min Sci. & Geomech. Abstr.* **18,** 1–21 (1981).
8. Mandelbrot B. *Fractal Geometry of Nature*, p. 468. Freeman, San Francisco (1982).
9. Brown E. T. (Ed.). *Rock Characterization Testing and Monitoring, ISRM Suggested Methods*, p. 211. Pergamon Press, Oxford (1981).
10. Turk N., Greig M. J., Dearman W. R. and Amin F. P. Characterization of rock joint surfaces by fractal dimension. *Proc. 28th U.S. Rock Mech. Symp.*, pp. 1223–1236 (1987).
11. Sakellariou M., Nakos B. and Mitsakaki C. The fractal dimension of rock discontinuities. Application in geophysics. *1st Hellenic Geophysical Congr.*, Athens, Greece (1989).
12. Maerz N. H. and Franklin J. A. Roughness scale effects and fractal dimension. *ISRM Int. Workshop for Scale Effects in Rock Masses*, Loen, Norway (1990).
13. Muralha J. and Charrna-Graca J. G. An experience on the application of fractal theory to basic shear strength studies. *ISRM-Sponsored Regional Symp. for Rock Joints*, Loen, Norway (1990).
14. Lee Y. H., Carr J. R., Barr D. J. and Haas C. J. The fractal dimension as a measure of the roughness of rock discontinuity profiles. *Int. J. Rock Mech. Min. Sci. & Geomech. Abstr.* **27,** 453–464 (1980).
15. Feder J. *Fractals*, p. 283, Plenum Press, New York (1988).
16. Mandelbrot B. B. Self-affine fractals and fractal dimension. *Phys. Scripta* **32,** 257–260 (1985).
17. Mandelbrot B. B. Self-affine fractal sets I–III. In *Fractals in Physics* (Trieste, 1985), (Edited by L. Pietronero and E. Tossati), p. 476. North-Holland, Amsterdam (1986).
18. Voss R. F. In *The Science of Fractal Images* (Edited by H. O. Peitgen and D. Saupe), p. 312. Springer, Berlin (1988).
19. Nakos B. Digital representation of cartographic phenomena based on fractal geometry theory. Application on Terrain's relief using digital models, p. 200. Dr Engng Thesis, National Technical Univ. of Athens, Greece (1990) (in Greek).
20. Voss R. F. Random fractals: self-affinity in noise, music, mountains and clouds. In *Fractals in Physics* (Edited by A. Aharony and J. Feder). *Physica D.* **38,** 362–371 (1989).
21. Maerz N. H., Franklin J. A. and Bennett C. P. Joint roughness measurement using shadow profilometry. *Int. J. Rock Mech. Min. Sci. & Geomech. Abstr.* **27,** 329–343 (1990).
22. Goff J. A. and Jordan T. H. Stochastic modeling of seafloor morphology: inversion of sea beam data for second-order statistics. *J. Geophys. Res.* **93,** 13,589–13,608 (1988).
23. Walpole R. E. and Myers R. H. *Probability and Statistics for Engineers and Scientists*, 2nd Edn, p. 580. MacMillan, New York (1978).
24. Newland D. E. *An Introduction to Random Vibration and Spectral Analysis*, p. 285. Longman, London (1975).
25. Berry M. V. and Lewis Z. V. On the Weierstrass–Mandelbrot fractal function. *Proc. R. Soc. Lond. A* **370,** 459–484 (1980).